

Electronic Supplementary Information (ESI)

A facile approach to construct organic D- π -A dyes via sequential condensation reactions for dye-sensitized solar cells

Hongjin Chen¹, Ashraful Islam^{2*}, Towhid H. Chowdhury², Idriss Bedja³, Hamid M. Ghaithan³, Rui Zhang¹, and Jian Liu^{1*}

1. Jiangsu Co-Innovation Center of Efficient Processing and Utilization of Forest Resources, College of Chemical Engineering, Nanjing Forestry University, Nanjing 210037, China.

2. Photovoltaic Materials Group, National Institute for Materials Science (NIMS), 1-2-1 Sengen, Tsukuba, Ibaraki 305-0047, Japan

3. Cornea Research Chair, Optometry Department, College of Applied Medical Sciences, King Saud University, Riyadh 11433, Saudi Arabia

E-mail: Islam.Ashraful@nims.go.jp, liu.jian@njfu.edu.cn

General

All chemicals and reagents were used as received from chemical company (Aldrich) without further purification. Column chromatography was performed using with silica gel (200 ~300 mesh) as a stationary phase. Cyclic voltammetry (CV) was performed on a CHI760E Electrochemical Workstation (CHI Instruments Co., Shanghai, China). All CV measurements were carried out in anhydrous CH₂Cl₂ containing 0.1 M TBAHFP as a supporting electrolyte, purging with argon prior to conduct the experiment. Platinum electrode was used as a working electrode, Ag/AgCl in saturated KCl (aq.) as a reference electrode, and a platinum wire as a counter electrode. UV-Vis spectra were measured in CH₂Cl₂ solution or TiO₂ film using UV-3600 Spectrophotometer (SHIMADZU). Fluorescence spectra were measured using FL6500 spectrophotometer (PerkinElmer). The ¹H- and ¹³C-NMR measurements were performed by a DRX spectrometer (Bruker BioSpin). Mass spectra were measured on a Shimadzu Biotech matrix-assisted laser desorption ionization (MALDI) mass

spectrometer. Geometry optimization and Molecular orbital distributions of three dyes were performed using B3LYP functional and 6-31G (d,p) basis set implemented in the Gaussian 09 program package.¹ To estimate the dye-loading amount of each dye in DSSCs, dyes were desorbed from the nanocrystalline TiO₂ film by dipping in 0.1 M TBAOH solution of 1: 1 mixture of H₂O and ethanol. The content of uptake dye was estimated from the absorption peak of each resulting solution.

Cell fabrication and characterization

The device fabrication was performed as follows. TiO₂ paste was received from dyesol Ltd. A double-layered TiO₂ film as photoanode containing 11 μm main transparent layer with ca. 20 nm sized titania particles and a 5 μm scattering layer with ca. 400 nm sized titania particles were screen printed on the fluorine-doped tin oxide (FTO) conducting glass substrate (~10 Ohm⁻², Solaronix). The double-layered films were heated to 520 °C and sintered for 1 hour and then cooled to 80 °C, following additional treatment with 0.1 M HCl aqueous solution. The resulted TiO₂ films were washed, dried and then dipped into a 3 × 10⁻⁴ M acetonitrile/n-BuOH (1/1, v/v) solution of the corresponding sensitizer in CH₃CN/n-BuOH (1/1, v/v) for 40 h. Afterwards, the dye-loaded TiO₂ film and a platinum coated conducting glass were assembled into a DSSC of a sandwich type and sealed by heating the Surlyn spacer (40 mm thick). An electrolyte consisting of 0.6 M dimethylpropylimidazolium iodide, 0.05 M I₂, 0.1 M LiI and 0.7 M TBP in acetonitrile was injected into the spacer from the counterelectrode side through a pre-drilled hole, and then the hole was sealed with a Bynel sheet and a thin-glass-slide cover by heating.

The *J-V* characteristics were carried out by using a black metal mask with an aperture area of 0.2304 cm⁻² under standard AM 1.5 sunlight, 100 mW·cm⁻² (WXS-155S-10: Wacom Denso Co. Japan). Monochromatic IPCE spectra were determined with monochromatic incident light of 1 × 10¹⁶ photons per cm² under 100 mW·cm⁻² in director current mode (CEP-2000BX, Bunko-Keiki). The IMVS were characterized with a potentiostat (Solartron1287) equipped with a frequency response analyzer

(Solartron1255B) at an open-circuit condition based on a monochromatic illumination (420 nm) controlled by a Labview system to obtain the photovoltaic response induced by the modulated light.

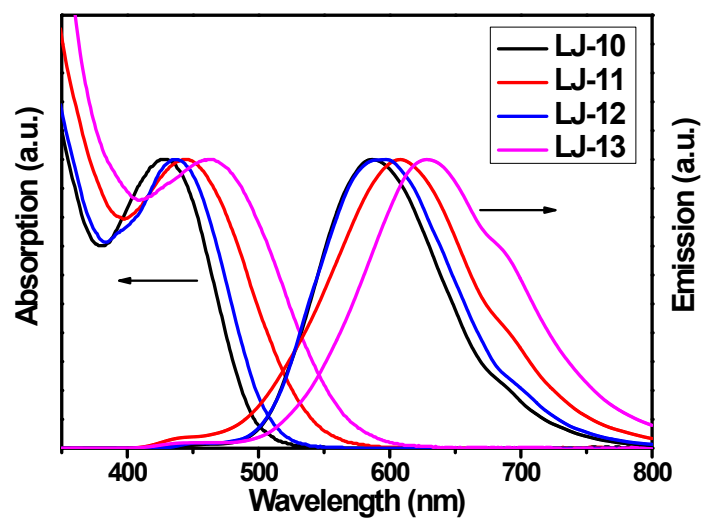


Fig. S1 Normalized UV-Vis and emission spectra of dyes **LJ-10**, **LJ-11**, **LJ-12** and **LJ-13** in CH_2Cl_2 .

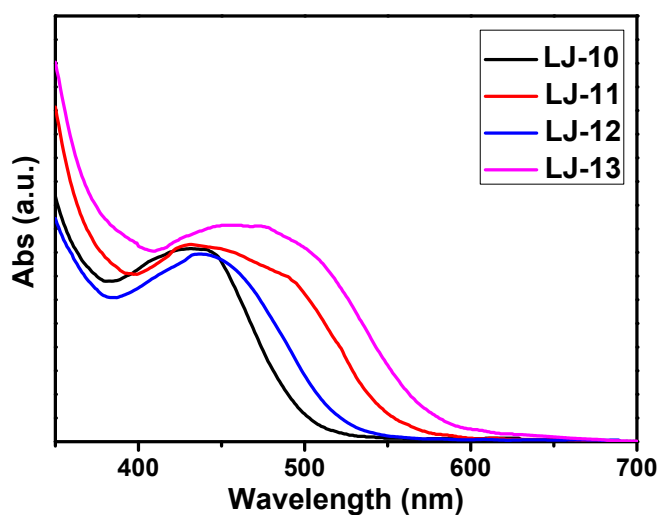


Fig. S2 Absorption spectra of dyes **LJ-10**, **LJ-11**, **LJ-12** and **LJ-13** anchored on a transparent TiO_2 films.

DFT Calculation

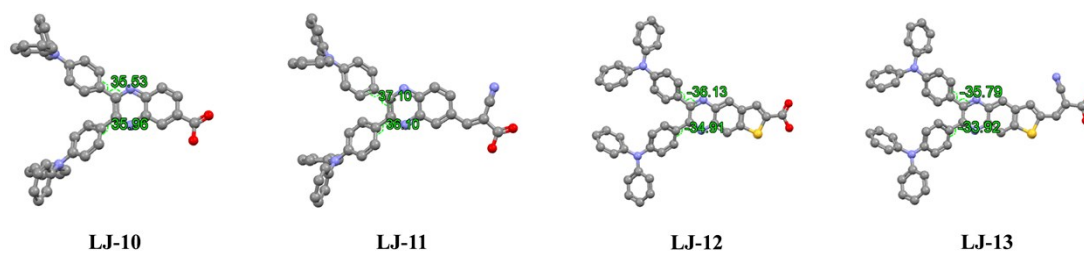


Fig. S3 Optimized ground-state geometries of dyes **LJ-10**, **LJ-11**, **LJ-12** and **LJ-13**.

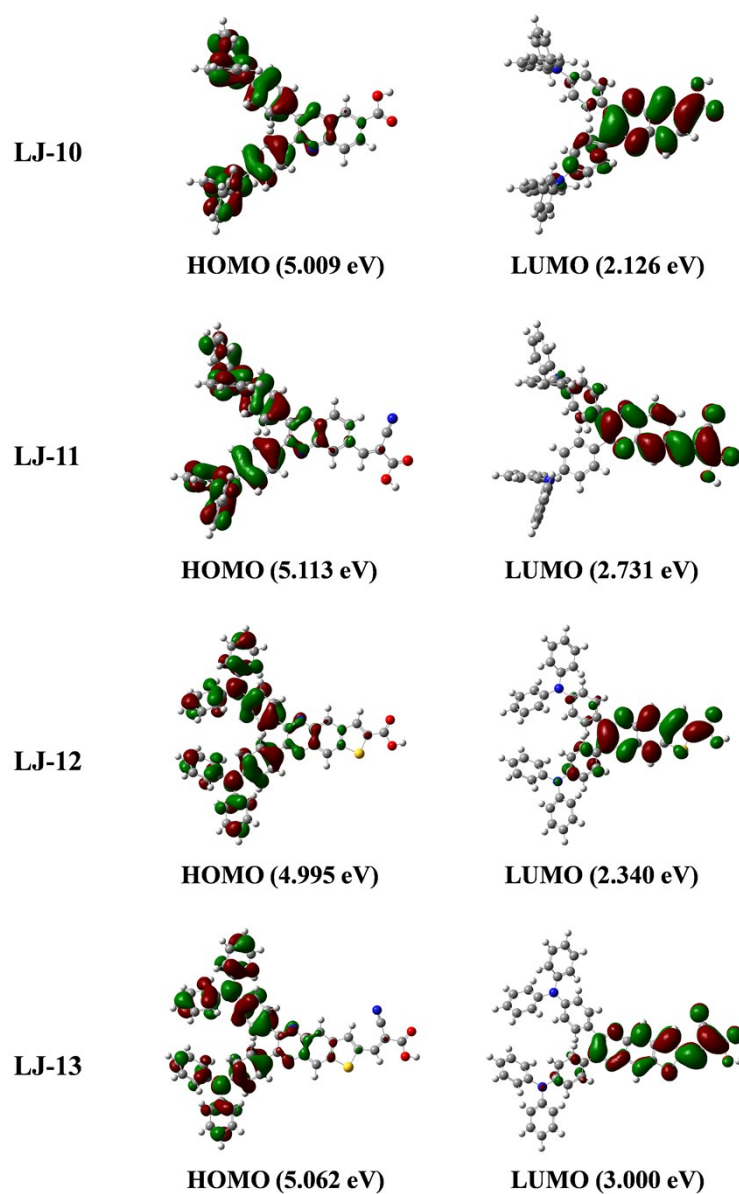


Fig. S4 The HOMO and LUMO of dyes **LJ-10**, **LJ-11**, **LJ-12** and **LJ-13** calculated at B3LYP/6-31G** level.

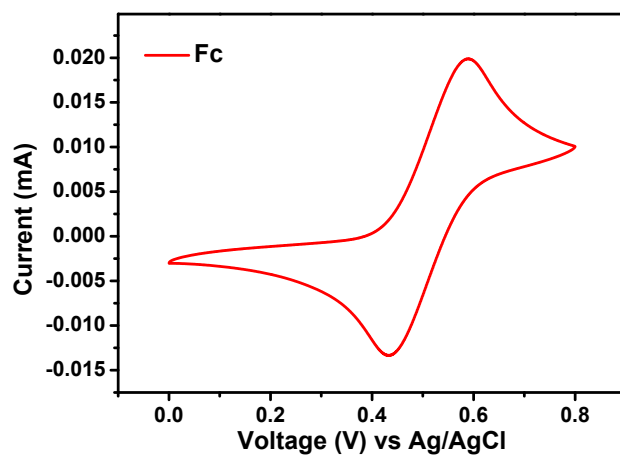


Fig. S5 Cyclic voltammograms of ferrocene in $\text{CH}_2\text{Cl}_2/\text{TBAHFP}$ (0.1 M), $[c] = 1 \times 10^{-4} \text{ mol}\cdot\text{L}^{-1}$, 293 K, scan rate = $100 \text{ mV}\cdot\text{s}^{-1}$.

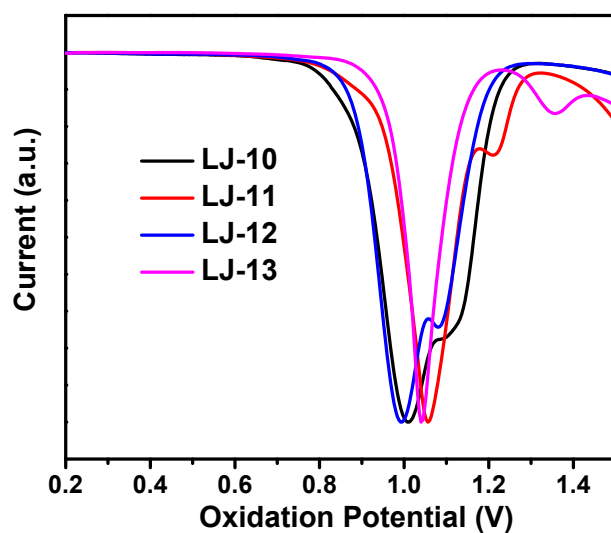


Fig. S6 Differential pulse voltammetry of dyes LJ-10, LJ-11, LJ-12 and LJ-13.

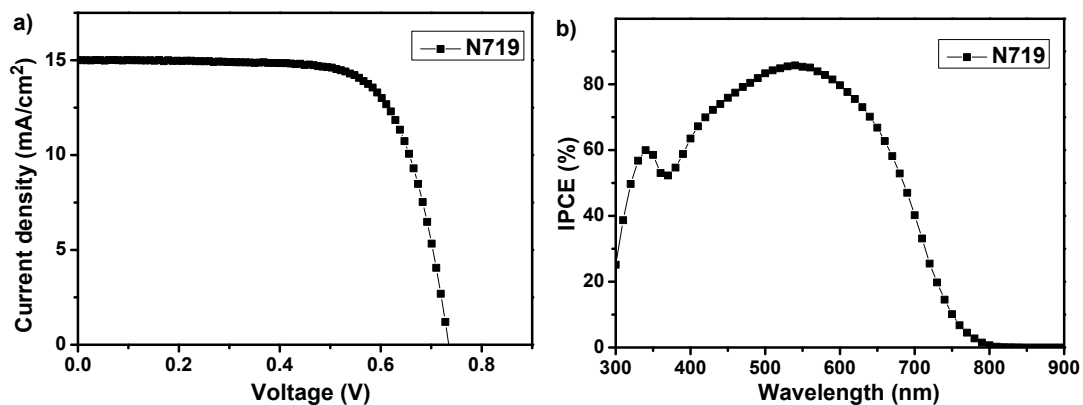


Fig. S7 J - V curve (a) and IPCE (b) of DSSC based on dye N719.

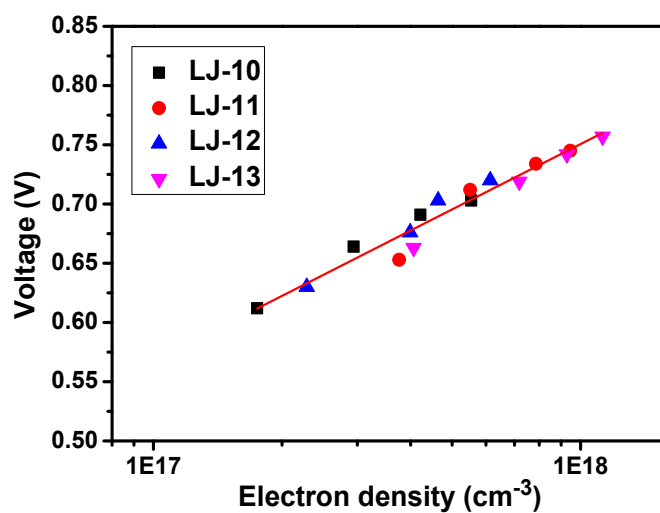


Fig. S8 V_{OC} as a function of extracted electron density for DSSCs based on dyes LJ-10, LJ-11, LJ-12 and LJ-13, respectively.

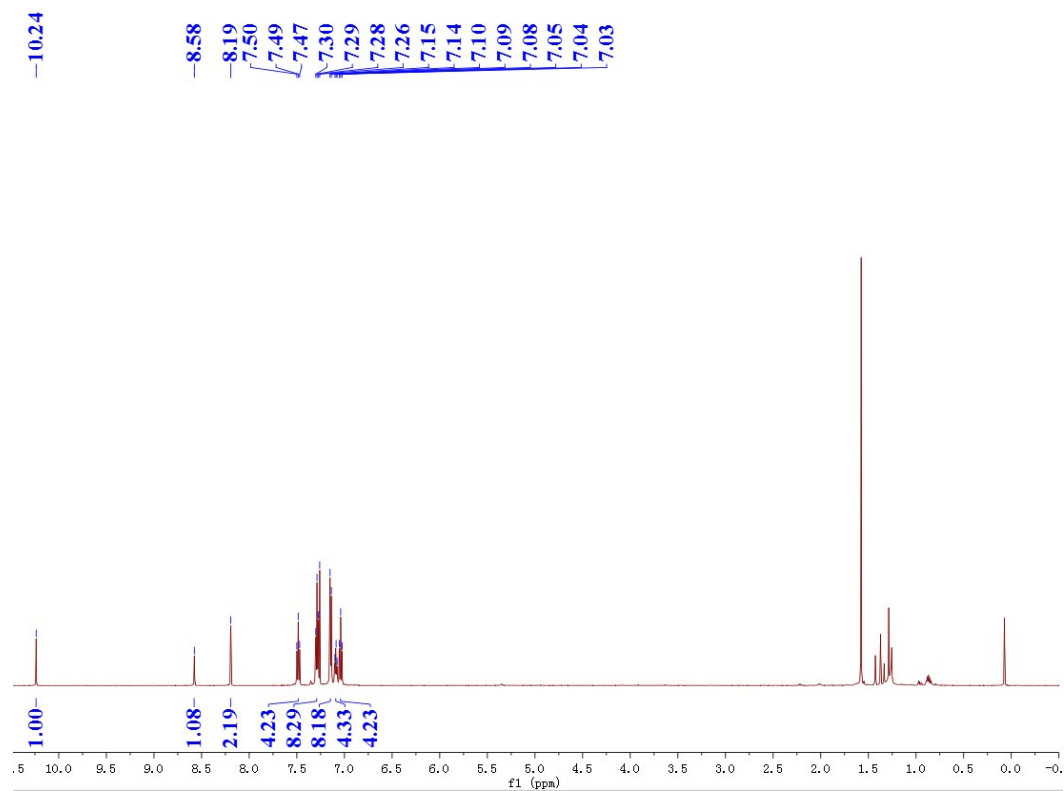


Fig. S9 ^1H NMR spectra of compound **3a**.

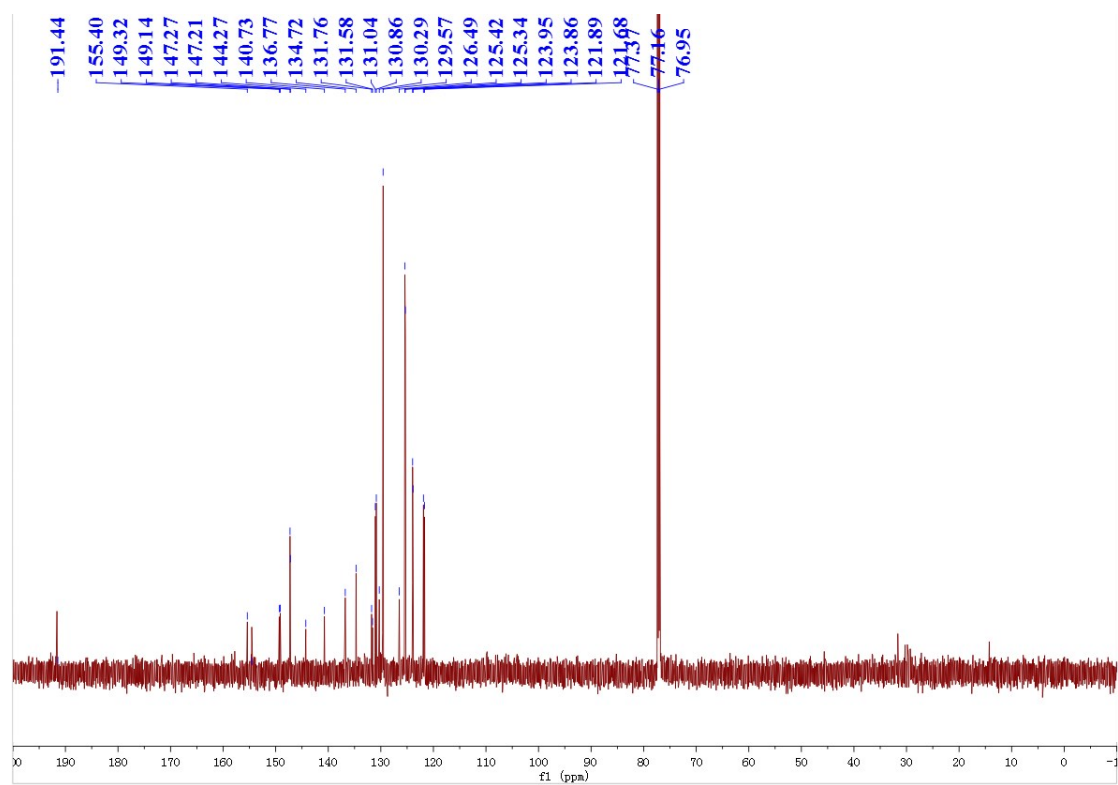


Fig. S10 ^{13}C NMR spectra of compound **3a**.

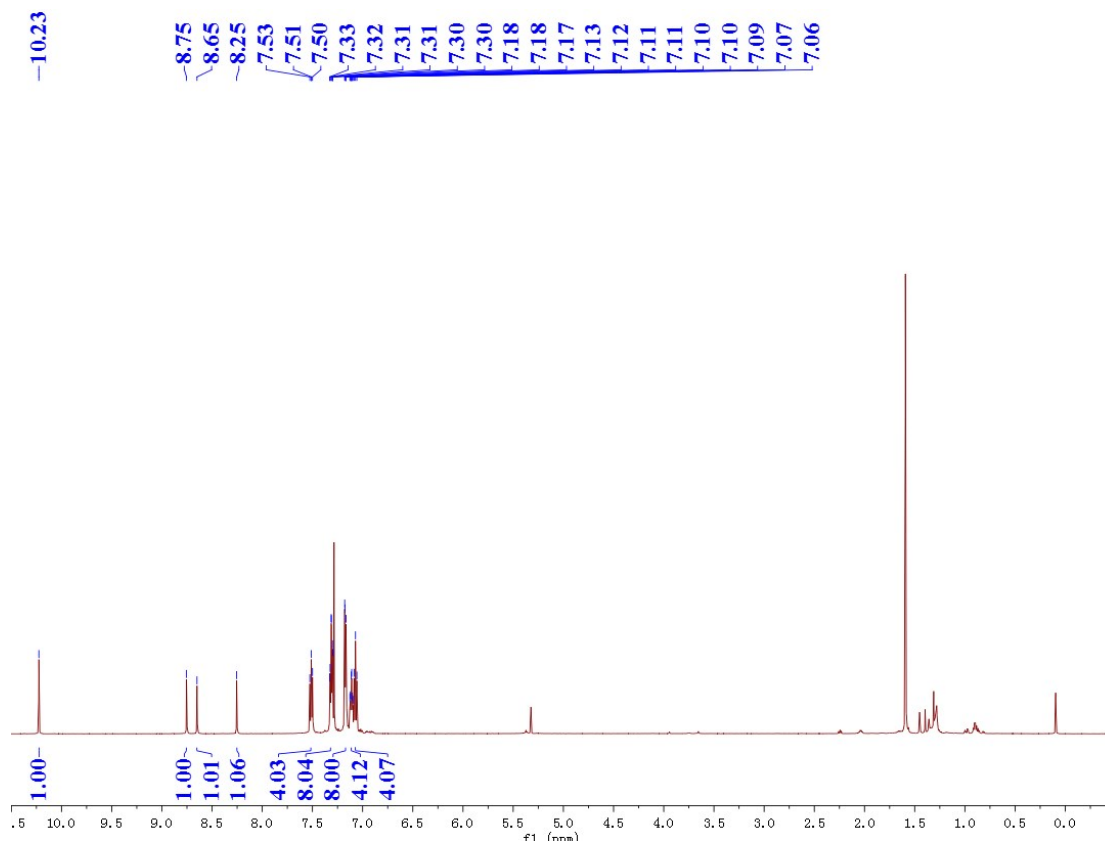


Fig. S11 ^1H NMR spectra of compound **3b**.

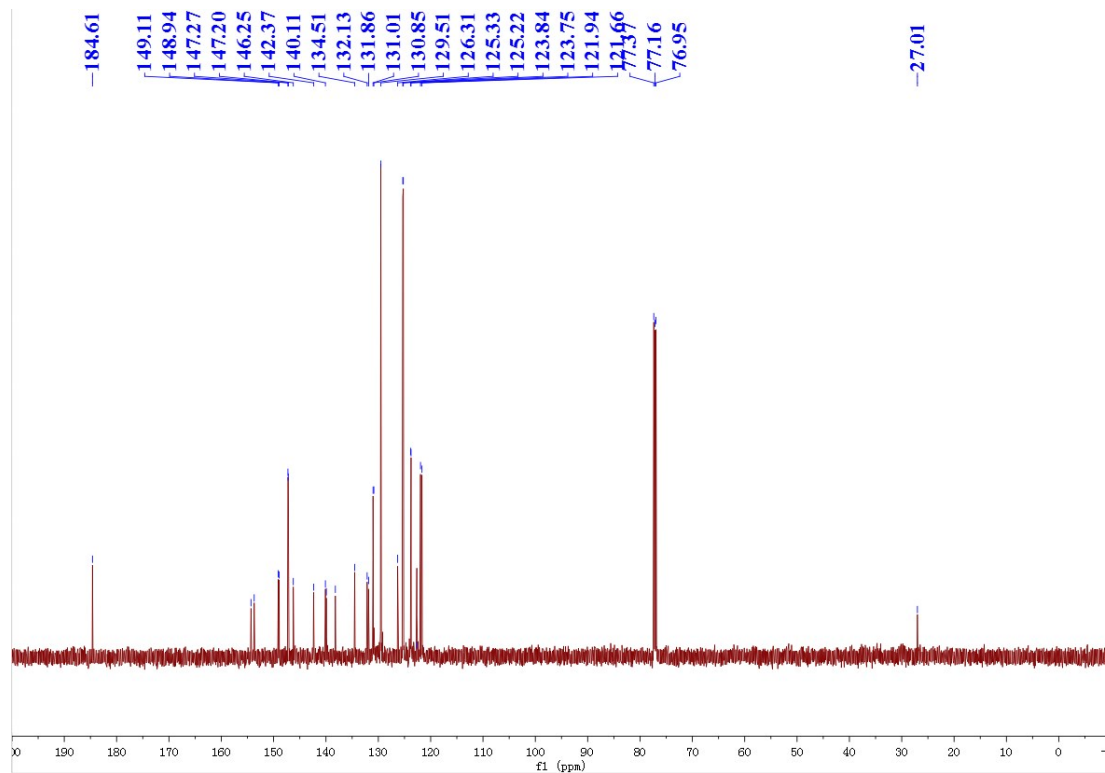


Fig. S12 ^{13}C NMR spectra of compound **3b**.

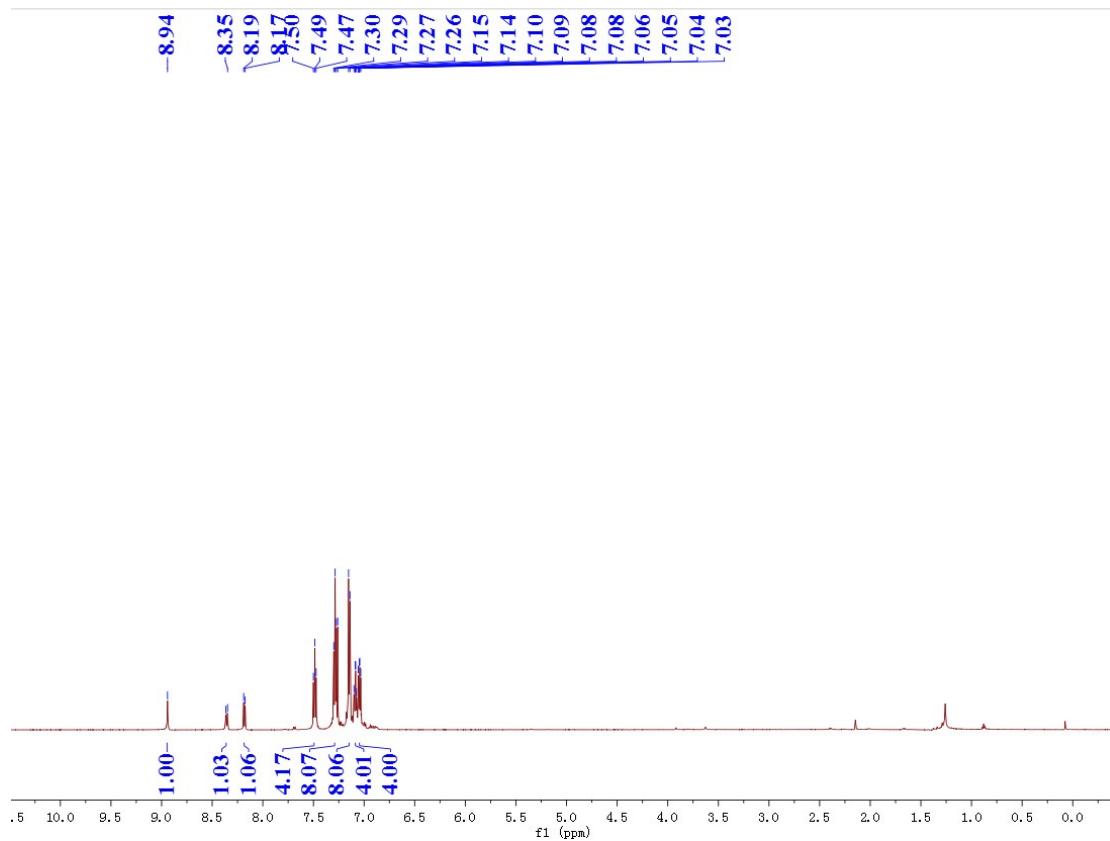


Fig. S13 ^1H NMR spectra of dye LJ-10.

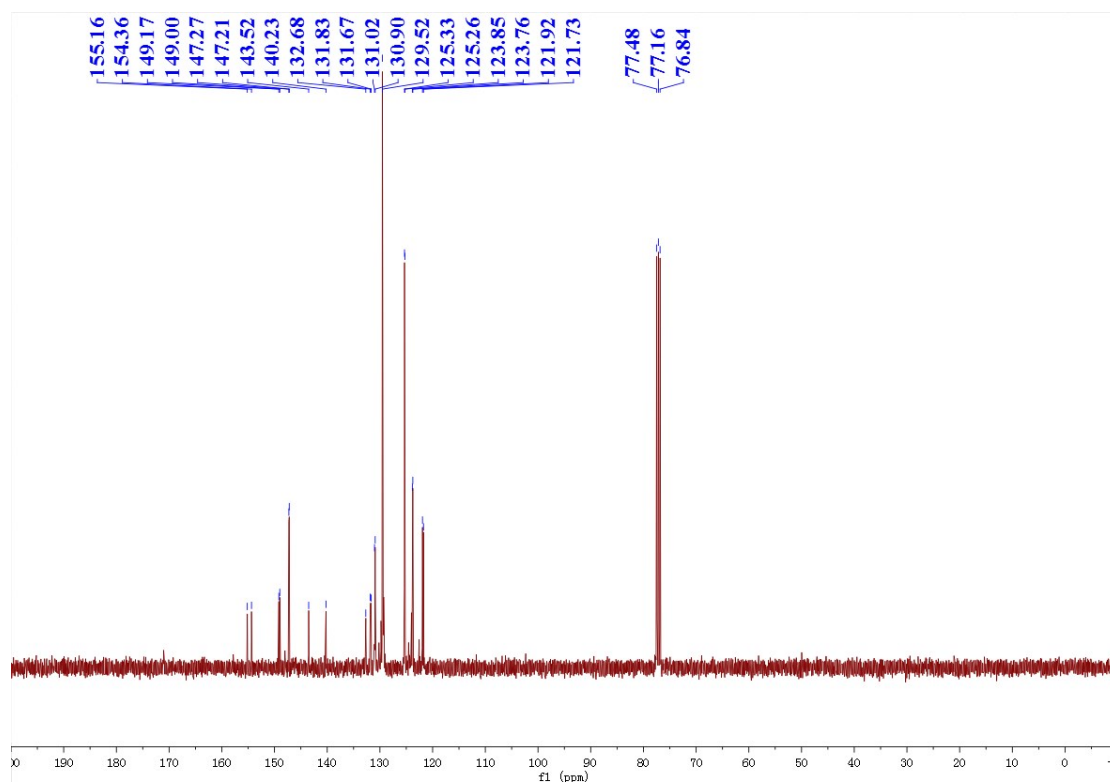


Fig. S14 ^{13}C NMR spectra of dye LJ-10.

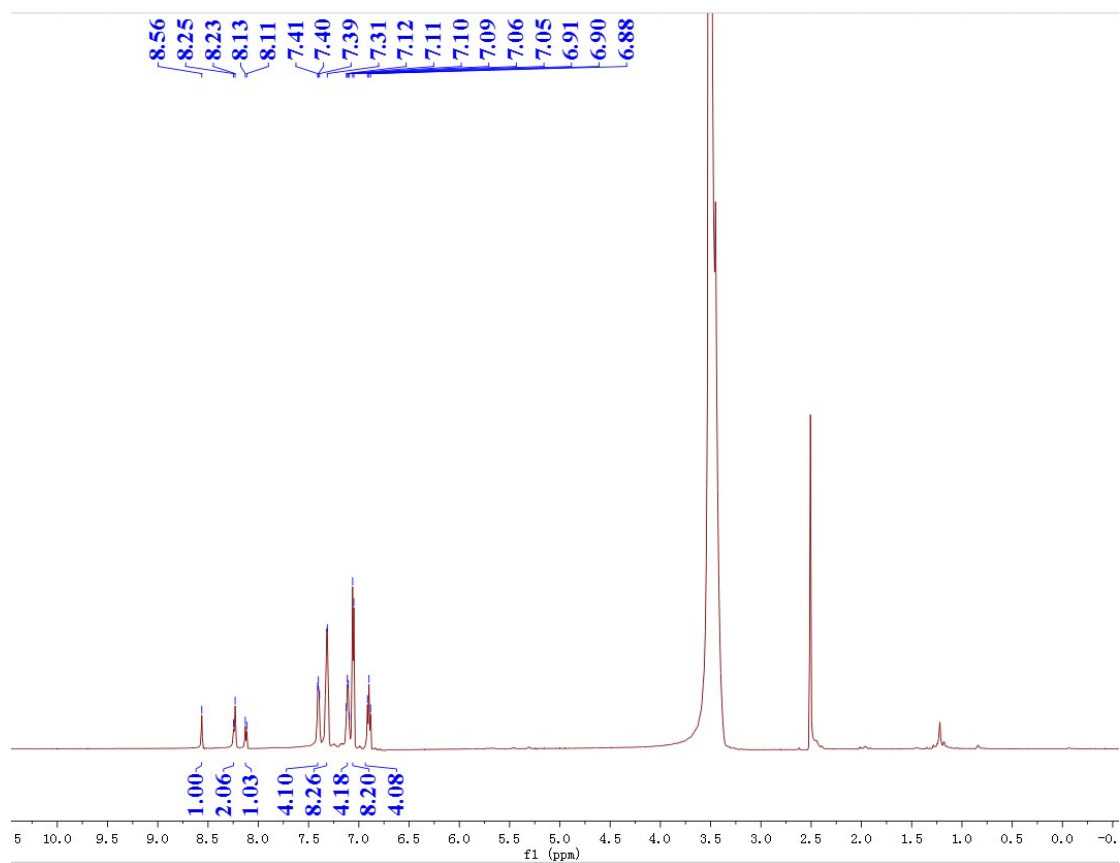


Fig. S15 ^1H NMR spectra of dye LJ-11.

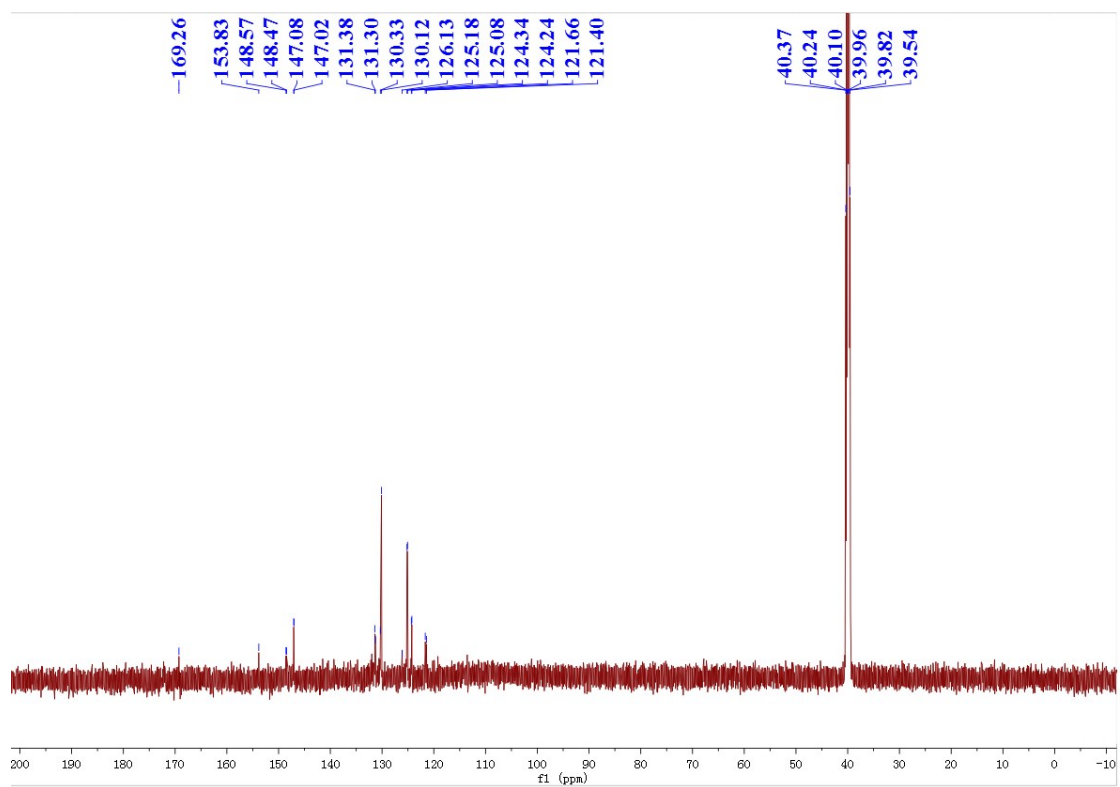


Fig. S16 ^{13}C NMR spectra of dye LJ-11.

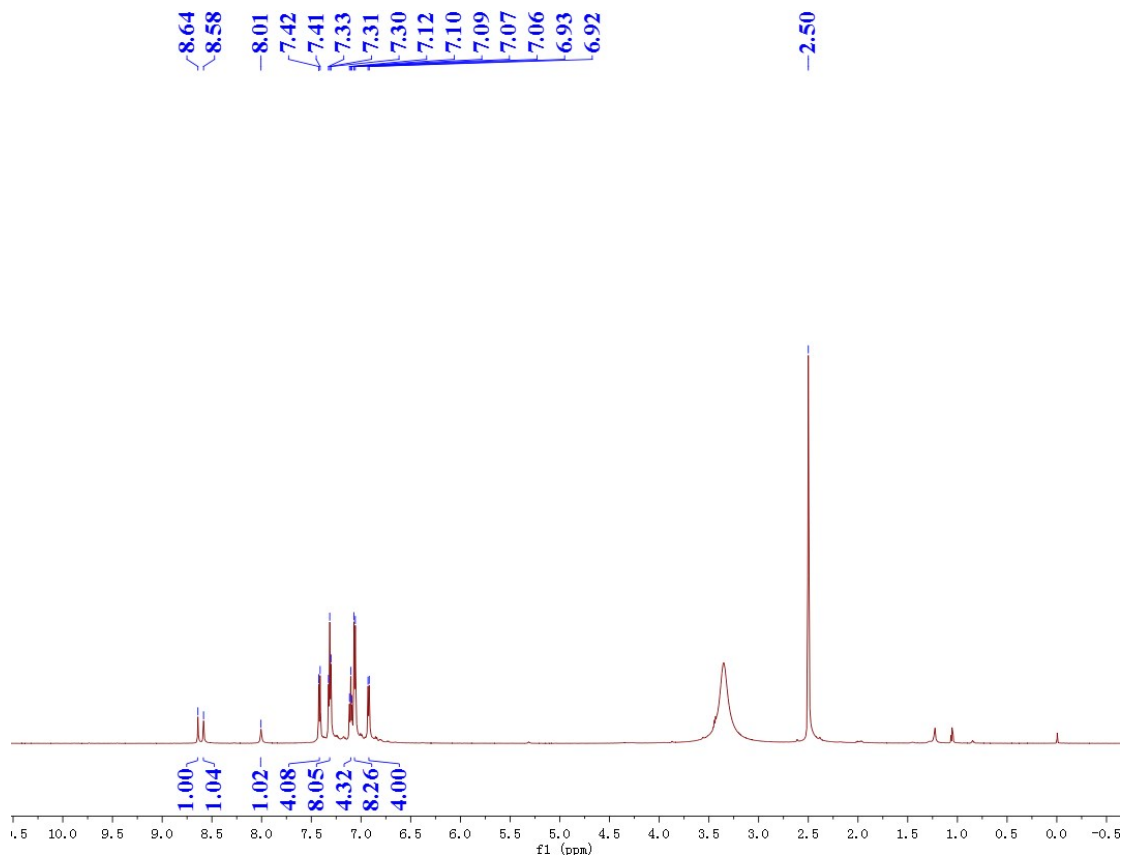


Fig. S17 ^1H NMR spectra of dye LJ-12.

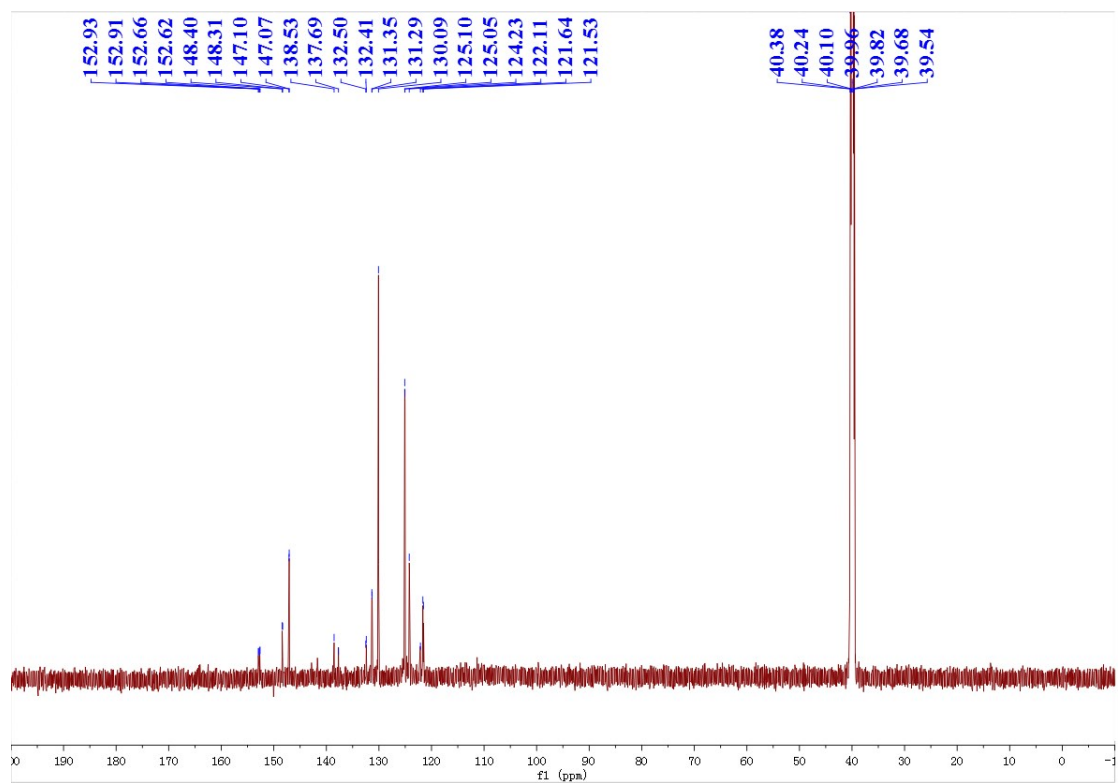


Fig. S18 ^{13}C NMR spectra of dye LJ-12.

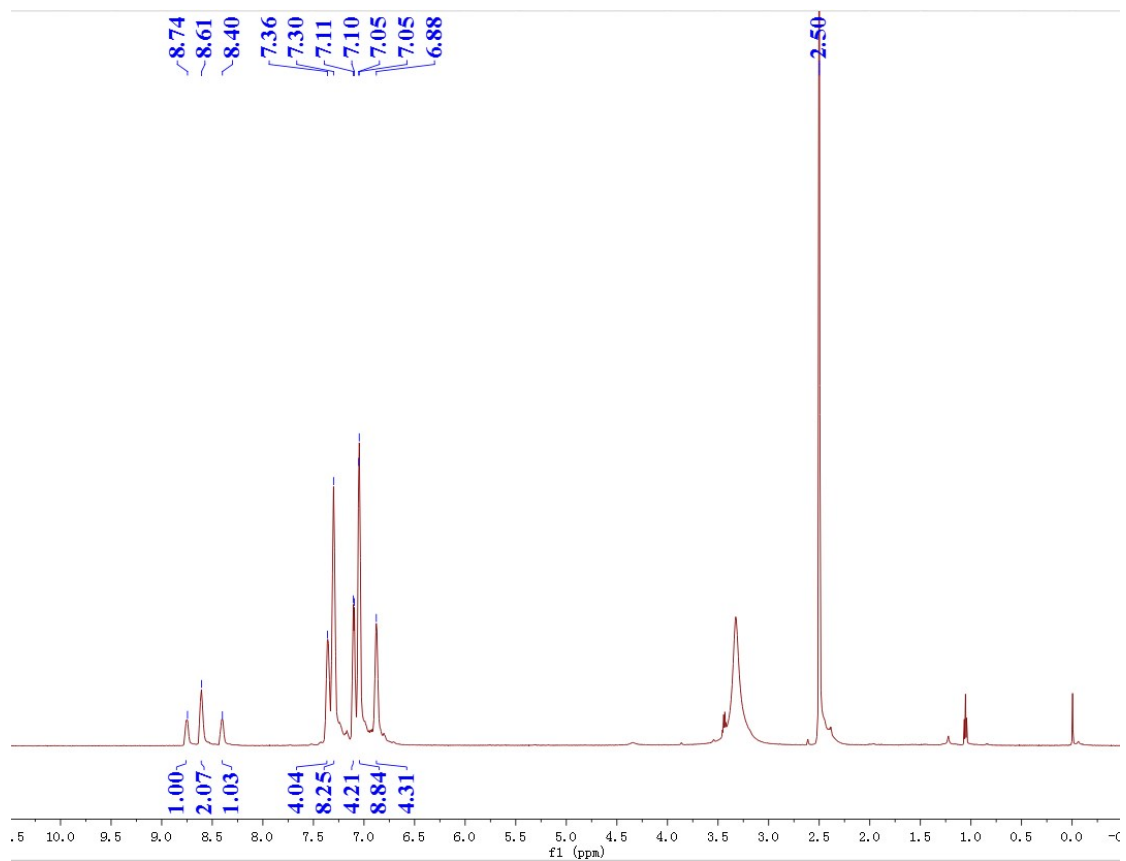


Fig. S19 ^1H NMR spectra of dye LJ-13.

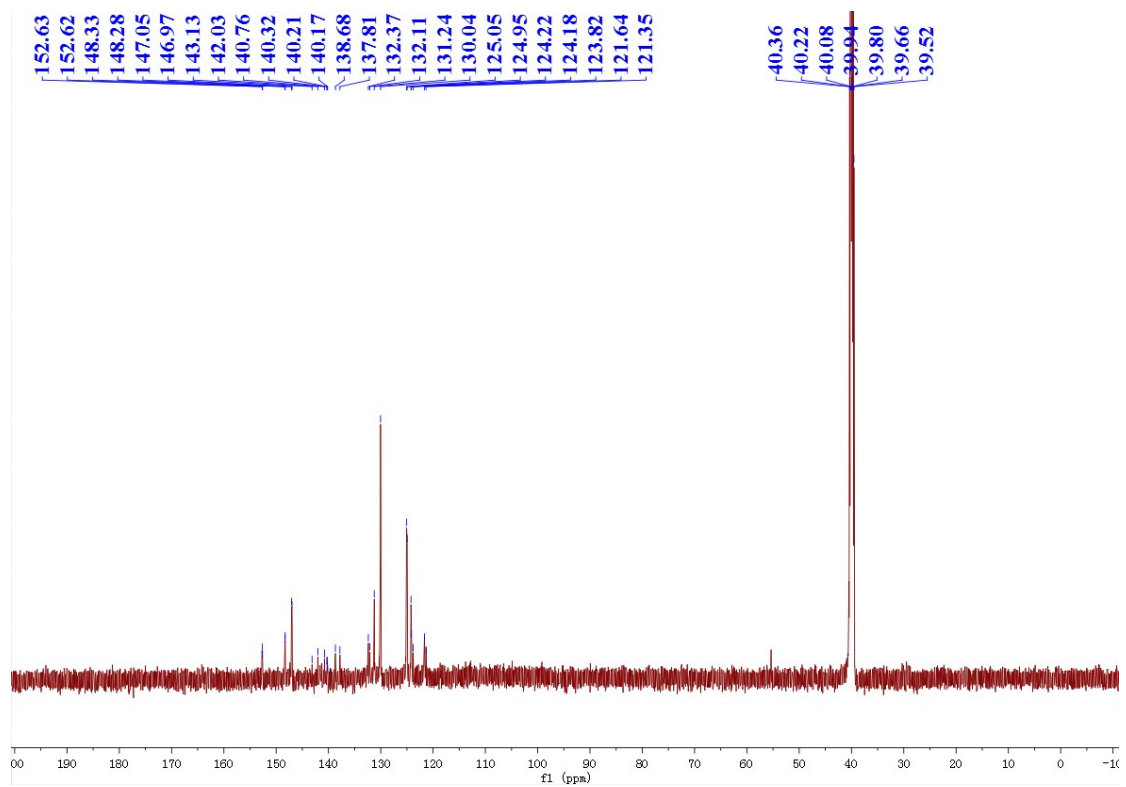


Fig. S20 ^{13}C NMR spectra of dye LJ-13.

Reference

1. M. J. Frisch, G. W. Trucks, H. B. Schlegel, G. E. Scuseria, M. A. Robb, J. R. Cheeseman, G. Scalmani, V. Barone, B. Mennucci, G. A. Petersson, H. Nakatsuji, M. Caricato, X. Li, H. P. Hratchian, A. F. Izmaylov, J. Bloino, G. Zheng, J. L. Sonnenberg, M. Hada, M. Ehara, K. Toyota, R. Fukuda, J. Hasegawa, M. Ishida, T. Nakajima, Y. Honda, O. Kitao, H. Nakai, T. Vreven, J. A. Montgomery Jr., J. E. Peralta, F. Ogliaro, M. Bearpark, J. J. Heyd, E. Brothers, K. N. Kudin, V. N. Staroverov, R. Kobayashi, J. Normand, K. Raghavachari, A. Rendell, J. C. Burant, S. S. Iyengar, J. Tomasi, M. Cossi, N. Rega, J. M. Millam, M. Klene, J. E. Knox, J. B. Cross, V. Bakken, C. Adamo, J. Jaramillo, R. Gomperts, R. E. Stratmann, O. Yazyev, A. J. Austin, R. Cammi, C. Pomelli, J. W. Ochterski, R. L. Martin, K. Morokuma, V. G. Zakrzewski, G. A. Voth, P. Salvador, J. J. Dannenberg, S. Dapprich, A. D. Daniels, O. Farkas, J. B. Foresman, J. V. Ortiz, J. Cioslowski and D. J. Fox, Gaussian 09, Revision A.02; Gaussian, Inc.: Wallingford, CT, **2009**.